International Journal of Computational and Experimental Science and ENgineering (IJCESEN)

Vol. 11-No.3 (2025) pp. 5768-5776
http://www.ijcesen.com

ISSN: 2149-9144

Research Article

Enhancing Machine Learning Approach for MGMT Promoter Methylation Detection in Glioma from MRI Features

Youssef Boulkhiout[1]*, Abdelouahab Moussaoui [2], Khaled Nasri [3]

[1]Department of Computer Science, Faculty of Sciences, University Setif 1 - Ferhat Abbas, Setif, 19000, Algeria
* **Corresponding Author Email:** youssef.boulkhiout@univ-setif.dz - **ORCID:** 0000-0002-5469-3442

[2]Department of Computer Science, Faculty of Sciences, University Setif 1 - Ferhat Abbas, Setif, 19000, Algeria
Email: abdelouahab.moussaoui@univ-setif.dz - **ORCID:** 0000-0003-3669-1264

[3]Department of Computer Science, Faculty of Sciences, University Setif 1 - Ferhat Abbas, Setif, 19000, Algeria
Email: nasri.khaled@univ-setif.dz - **ORCID:** 0009-0002-0217-9625

Article Info:

DOI: 10.22399/ijcesen.3610
Received : 16 June 2025
Accepted : 01 August 2025

Keywords

Radiogenomics
Glioblastoma
MGMT methylation
Artificial intelligence
Machine learning

Abstract:

Glioblastoma (GBM) is the most aggressive primary brain tumor in adults, marked by high recurrence rates and poor prognosis. The methylation status of the O-6-methylguanine-DNA methyltransferase (MGMT) gene promoter plays a critical role in determining treatment response and patient survival. This work provides non-invasive machine learning (ML) solution for prediction of MGMT methylation status using features of magnetic resonance imaging (MRI) scans, aiming to support personalized therapeutic strategies. The method involves a three-step pipeline: First, extraction of image features from multi-modal MR. Second, Selection of the most important common features using light gradient boosting machine (LightGBM) algorithm and categorical gradient boosting (CatBoost). then, a voting ensemble of multiple ML models is trained on the selected features to classify MGMT methylation. The model was developed using Brain Tumor Segmentation (BraTS) 2021 dataset, which includes both segmentation masks and MGMT annotations. Its performance was evaluated using accuracy, precision, sensitivity, specificity, and area under the receiver operating characteristic (ROC) curve (AUC). The model achieved an accuracy of 92.86% and AUC of 96.84%, demonstrating strong alignment with clinical outcomes and surpassing conventional methods. These findings highlight the effectiveness of features extraction from multi-modal MRI analysis, and ML-based classification for biomarker prediction. The approach offers a promising step forward in precision medicine for GBM, enabling more accurate and individualized treatment planning.

1. Introduction

GBM, classified as a grade IV astrocytoma by the World Health Organization [1], constitutes the most aggressive and predominant primary malignant brain tumor in adults, exhibits significant molecular heterogeneity, with MGMT promoter methylation status emerging as a pivotal biomarker for prognostic assessment and therapeutic response prediction [2]. MGMT methylation is associated with improved response to temozolomide chemotherapy, guiding personalized therapeutic strategies [3]. However, determining MGMT status traditionally requires invasive biopsy or surgical resection, posing risks to patients and delaying treatment decisions. Non-invasive prediction of MGMT status using MRI has emerged as a promising alternative, leveraging multi-sequence MRI scans (T1-weighted (T1W), T2-weighted (T2W), contrast-enhanced T1 (T1CE), and fluid-attenuated inversion recovery (FLAIR)) to capture tumor characteristics. Recent advances in machine learning have facilitated the development of robust models for medical image analysis, particularly in tumor segmentation and classification. The extraction of radiomics features is one of the best robust solutions in medical image analysis, by minimizing the size of complex imaging data, efficacity of data representation and analysis, and robustness to the noise effects. ML approaches have shown remarkable success in isolating tumor regions

and extracting relevant features from complex imaging data [4].

In this study, we present a novel ML-based framework for non-invasive prediction of MGMT methylation status using features extracted from multi-modal MRI scans from the Brain Tumor Segmentation 2021 dataset [5]. This dataset provides both annotated tumor segmentation masks and MGMT methylation labels, allowing for targeted analysis of tumor-specific regions. Our pipeline integrates radiomic feature extraction, feature selection via LightGBM and CatBoost algorithms, and final classification using an ensemble of 4 ML models—XGBoost, CatBoost, LightGBM, and RandomForest—combined through a voting mechanism. This comprehensive approach aims to enhance prediction accuracy and clinical relevance, offering a scalable and non-invasive solution for precision oncology in GBM patient management.

2. Related Works

The MGMT promoter methylation status is a critical biomarker in gliomas, impacting temozolomide response and survival. Invasive testing is hindered by cost, complexity, and tumor heterogeneity, spurring non-invasive radiomics and AI methods using MRI. This state-of-the-art review synthesizes 12 studies, reordered by predictive performance (accuracy or AUC), to evaluate methodologies and clinical potential for MGMT methylation prediction in gliomas.

Significant progress in radiomics and AI has been achieved, with studies demonstrating varied predictive accuracies. Sasaki et al. reported the MGMT prediction accuracy at 67% using LASSO regression with 489 texture features, though it excelled in survival stratification. Hajianfar et al. achieved an AUC of 0.78 with a Decision Tree classifier on MRI features, emphasizing edema region importance. Qian et al. reached 80% ± 10% accuracy using F-DOPA positron emission tomography (PET) with a random forest model, highlighting PET's complementary role. Tasci et al. obtained 81.6% accuracy with a hybrid feature weighting approach on multiparametric MRI, noting the need for external validation. Crisi et al. achieved an AUC of 0.84 with DSC-MRI perfusion features, effective for highly methylated GBM. Korfiatis et al. reported an AUC of 0.85 using T2-weighted MRI texture features with SVM and random forest classifiers. Han et al. achieved AUCs of 0.887 (training) and 0.760 (validation) for 1p/19q co-deletion prediction, suggesting broader radiomics applications. Karabacak et al. developed a ML approach LightGBM and random forest models for WHO grade II/III gliomas using the National Cancer Database, deployed in a web application with SHAP for interpretability. The test achieved by AUROC of 0.813–0.896 (grade II) and 0.855–0.878 (grade III). Do et al. achieved 75% accuracy using genetic algorithm-based feature selection, transferable to low-grade gliomas. Yu et al. set the highest benchmark at 0.923 AUC using a Transformer model, integrating intra-and peritumoral MRI features. Alternative modalities enhance prediction capabilities. Qian et al.'s PET-based approach and Crisi et al.'s DSC-MRI method complement traditional MRI, improving accuracy in complex cases. Jiang et al. (2024) fused multi-sequence MRI features (T1W, T1CE, FLAIR) to predict MGMT status in lower-grade gliomas, with an AUC of 0.761, underscoring the value of modality fusion. Kickingereder et al., outperformed clinical models in survival stratification using 12,190 radiomic features, while Karabacak et al.'s web application (AUROC 0.813–0.896) supports clinical integration with interpretable SHAP analysis.

Challenges include metric heterogeneity, External validation, emphasized by Tasci et al. and Han et al., is crucial for generalizability. Integrating clinical factors, as suggested by Kickingereder et al., could enhance performance. In conclusion, radiomics and AI, particularly machine learning, have revolutionized MGMT methylation prediction, with top accuracies exceeding 81% and AUCs exceeding 92.3%. Alternative modalities and standardized guidelines bolster reliability. Future efforts should prioritize validation, standardization, and clinical adoption to optimize glioma treatment and prognosis.

3. Material and Methods

The aim of this research is to develop a ML approach to predict the MGMT promoter methylation status in glioma patients using multi-sequence MRI scans from the BraTS 2021 dataset.

The next figure presents the pipeline illustrating the entire workflow adopted in this research, starting from data collection and preprocessing with the Brats2021 dataset, including 577 patients and 3D images (T1, T1ce, T2, FLAIR) with tumor segmentation, followed by radiomics feature extraction. It then proceeds through feature selection using LightGBM and CatBoost to select 15 common features for 559 patients, data normalization with standard scaler values in [-1, 1], and dataset splitting into train (475 patients, 85%) and test (84 patients, 15%) sets. The pipeline includes class balancing with SMOTE for methylated and unmethylated classes, data augmentation with a noise level of 0.03 and 100% of augmentation factor, and model training using an ensemble of CatBoost, XGBoost,

LightGBM, and Random Forest. Finally, it concludes with models testing, calculation of evaluation metrics, and plotting of results.

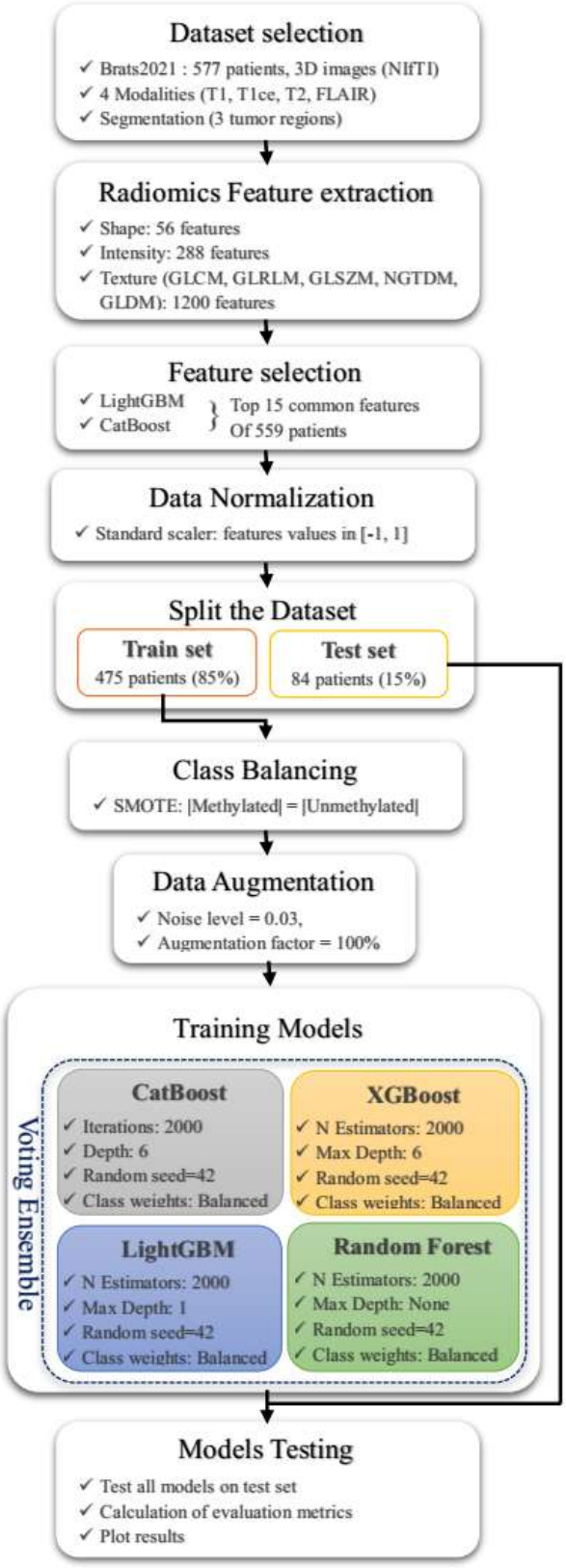

Figure 1. *The modeling Pipeline.*

3.1 Dataset Selection

Brats 2021 dataset includes tumor segmentation maps and MGMT promoter methylation status labels for patients, supporting two tasks. Task 1 focuses on tumor segmentation for 1,251 patients, while Task 2 predicts MGMT methylation status for 585 labeled patients and 87 unlabeled ones. Our analysis focuses on the 577 labeled patients common to both tasks which have 276 MGMT unmethylated and 301 methylated. Each patient's data consists of isotropic voxel images (240×240×155) across four modalities—T1W, T1CE, T2W, and FFLAIR—along with segmented masks combining tumor subregions: necrosis (label 1), enhancing tumor (label 2), and edema (label 4).

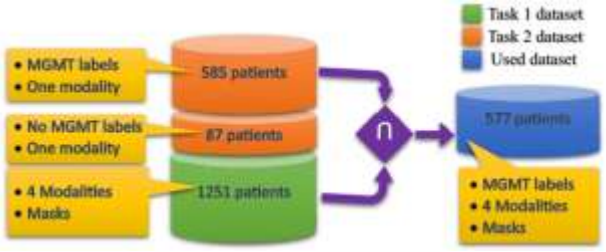

Figure 2. *Data selection from Brats 2021.*

3.2 Feature extraction

In this step, radiomics features are extracted from MRI scans for each patient across four modalities: T1W, T1CE, T2W, and FLAIR, covering all tumor subregions (necrosis, enhancing tumor, and edema). Three main categories of radiomics features are used: 1) Shape-based features, which characterize the 2D or 3D geometry and size of the tumor, such as volume, surface area, compactness, sphericity, elongation, flatness, maximum diameter, and surface-to-volume ratio; 2) Intensity-based features (first-order statistics), which describe voxel intensity distributions, including mean, median, standard deviation, skewness, kurtosis, entropy, and energy; and 3) Texture-based features (second-order and higher-order statistics), which capture spatial relationships and patterns among voxel intensities, including five subcategories: Gray Level Co-occurrence Matrix (GLCM), measuring pixel intensity pair frequency (contrast, correlation, homogeneity, energy, dissimilarity, angular second moment); Gray Level Run Length Matrix (GLRLM), quantifying consecutive voxels With consistent intensity, (short run emphasis, long run emphasis, gray level non-uniformity, run percentage); Gray Level Size Zone Matrix (GLSZM), detecting homogeneous region sizes (small area emphasis, large area emphasis, zone entropy); Neighboring Gray Tone Difference Matrix (NGTDM), evaluating intensity differences between a voxel and its neighbors (coarseness, contrast,

busyness, complexity); and Gray Level Dependence Matrix (GLDM), focusing on voxel dependencies with similar intensities (dependence non-uniformity, large dependence emphasis). Using PyRadiomics tools, 1544 radiomics features are extracted and organized into a CSV file as showed in the next table:

Table 1. *Radiomics Features distribution.*

Features		Per Modality	Per Region × (4 Modalities)	Total × (3 Regions + Whole)
Shape		-	14	56
Intensity		18	72	288
Texture	GLCM	24	96	384
	GLRLM	16	64	256
	GLSZM	16	64	256
	NGTDM	5	20	80
	GLDM	14	56	224
Grand Total		93	386	1544

The next figure shows the steps of radiomics features extraction from selected IRM scans and features selection:

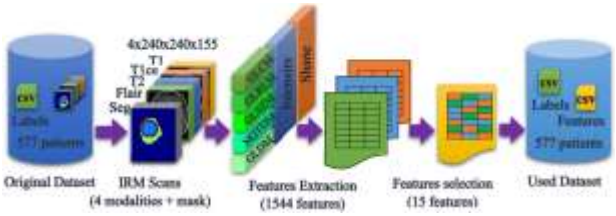

Figure 3. *Radiomics features extraction from IRM scans and features selection from csv file.*

3.3 Feature selection

Feature selection is a critical step in machine learning, aimed at enhancing model performance, reducing computational complexity, and improving interpretability by identifying the most impactful features for predictive modeling. A robust approach to feature selection involves leveraging the strengths of LightGBM and CatBoost, two powerful gradient-boosting algorithms known for their efficiency and accuracy in handling complex datasets. In this method, both LightGBM and CatBoost independently rank features based on their importance, which reflect each feature's contribution to the model's predictive power. By combining the insights from these algorithms, we select the top 15 features that consistently demonstrate high importance across both models, ensuring a consensus-driven approach to feature selection. The results of this feature selection process are presented in the next figure.

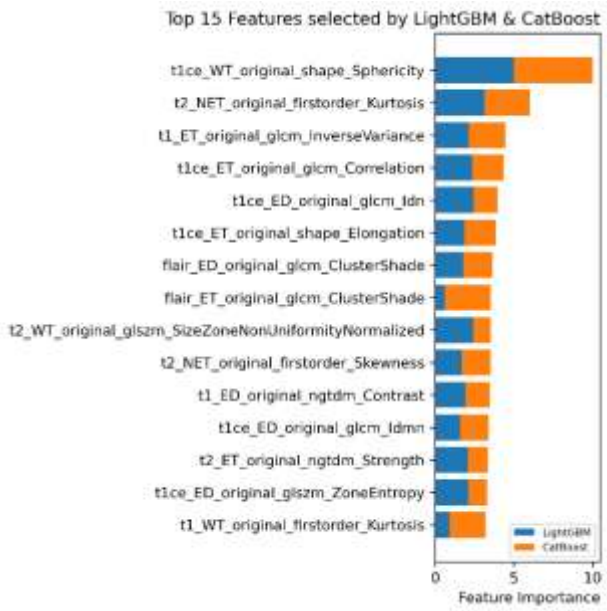

Figure 4. *Results of features selection steps using LightGBM and CatBoost.*

3.4 Dataset Splitting

The dataset used for predicting MGMT methylation status, stored as a CSV file, was meticulously preprocessed to ensure data quality and reliability. In the first step, all rows and columns containing multiple missing values were removed to eliminate incomplete or unreliable data points. Additionally, duplicate columns were identified and eliminated to avoid redundancy, resulting in a refined dataset comprising 1530 features across 490 patients. Then, the dataset was divided into training (85%) and test (15%) sets using stratified sampling. This approach ensured that the distribution of MGMT methylation status, a critical binary outcome, remained balanced across both subsets, preserving the representativeness of the data as showed in the next figure.

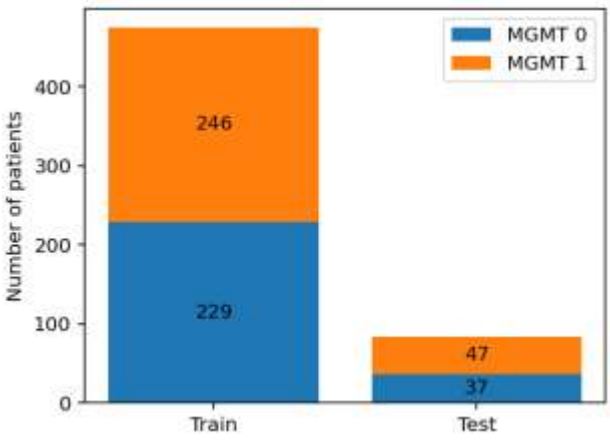

Figure 5. *Dataset distribution over subsets.*

3.5 Data Normalization

In this step, all feature values in the dataset were converted to the float32 data type to ensure computational efficiency and consistency across numerical operations. Then, the features were normalized using the Standard Scaler to transform their values to a standardized range of [-1, 1]. This normalization process centers the data by subtracting the mean and scaling it by the standard deviation, ensuring zero mean and one variance, which stabilizes machine learning algorithms and accelerates training convergence. The formula for transforming a feature x is given by:

$$x_{Normalized} = \frac{x-\mu}{\sigma} \qquad (1)$$

where: x is the original feature value, μ is the mean of the feature, and σ is the standard deviation of the feature.

3.6 Class Balancing

To address class imbalance in the MGMT methylation status classification task, we utilized the Synthetic Minority Over-sampling Technique (SMOTE). This technique generates synthetic samples for the minority class by interpolating between existing samples and their nearest neighbors, resulting in a balanced training subset distribution. By augmenting the representation of the minority class, SMOTE optimizes the training process, thereby enhancing the efficacy of machine learning models..

3.7 Data Augmentation

To improve model generalization and mitigate the challenges of a limited dataset, we employed data augmentation by injecting controlled noise into the training sub-dataset. This approach enhances the diversity of training samples while preserving the semantic integrity of the data. By introducing subtle variations, this technique reduces the risk of overfitting, thereby enhancing the robustness and stability of the machine learning models.

3.8 Evaluation Metrics

The performance of the models was evaluated on the test subset using several metrics, including accuracy, precision, area under the receiver operating characteristic curve (AUC-ROC), F1 score, and Cohen's Kappa. Additionally, we generated plots to visualize the evaluation accuracy, AUC, as well as the ROC curve and confusion matrix for the test set.

- **Accuracy**: Quantifies the overall precision of predictive outcomes in a model.

$$\text{Acc} = \frac{\text{TP} + \text{TN}}{\text{TP} + \text{TN} + \text{FP} + \text{FN}} \qquad (2)$$

Where: TP = True Positives, TN = True Negatives, FP = False Positives, FN = False Negatives

- **F1 Score**: The harmonic means of precision and recall, useful for imbalanced datasets.

$$\text{F}_1 \text{ score} = \frac{2\times\text{Precision}\times\text{Recall}}{\text{Precision}+\text{Recall}} \qquad (3)$$

Where:

$$\text{Precision} = \frac{\text{TP}}{\text{TP} + \text{FP}} \qquad (4)$$

$$\text{Recall} = \frac{\text{TP}}{\text{TP} + \text{FN}} \qquad (5)$$

- **AUC-ROC**: Measures the model's ability to distinguish between classes. The ROC curve plots the relationship between True Positive Rate (TPR called Recall) and False Positive Rate (FPR):

$$\text{FPR} = \frac{\text{FP}}{\text{FP} + \text{TN}} \qquad (6)$$

AUC is the area under this curve, typically calculated using the trapezoidal rule.

- **Cohen's Kappa**: Evaluates classification agreement between predicted and actual labels, adjusting for chance.

$$\kappa = \frac{\text{P}_0 - \text{P}_e}{1 - \text{P}_e} \qquad (7)$$

Where:

$$\begin{cases} \text{P}_0 = \frac{\text{TP}+\text{TN}}{\text{Total}} - OA \\ \text{P}_e = \frac{(\text{TP}+\text{FP})(\text{TP}+\text{FN})+(\text{FN}+\text{TN})(\text{FP}+\text{TN})}{\text{Total}^2} - EA \end{cases} \qquad (8)$$

OA: Observed agreement, EA: Expected agreement

- **Confusion Matrix**: is the table that summarizes prediction outcomes.

Table 2. *Confusion matrix.*

	Predicted Negative	**Predicted Positive**
Actual Negative	True Negative (TN)	False Positive (FP)
Actual Positive	False Negative (FN)	True Positive (TP)

3.9 Training Models

In this study, we trained four state-of-the-art machine learning models—CatBoost, XGBoost,

LightGBM, and Random Forest—on the augmented subset. These models were selected for their robust performance on tabular data and their ability to effectively capture complex feature interactions. Following individual model evaluation, we developed an ensemble approach that integrates the predictions of these models through a majority voting strategy. This voting-based ensemble capitalizes on the diverse strengths of the base models, enhancing prediction accuracy and robustness, particularly for the classification of MGMT methylation status.

4. Results And Discussions

In this study, we evaluated five machine learning models—CatBoost, XGBoost, LightGBM, Random Forest (RF), and a Voting Ensemble (VE)—on a binary classification task using a test set of 15 radiomics features. The feature selection process, justified in Figure 6, illustrates the accuracy and AUC for each model across varying counts of the most important features.

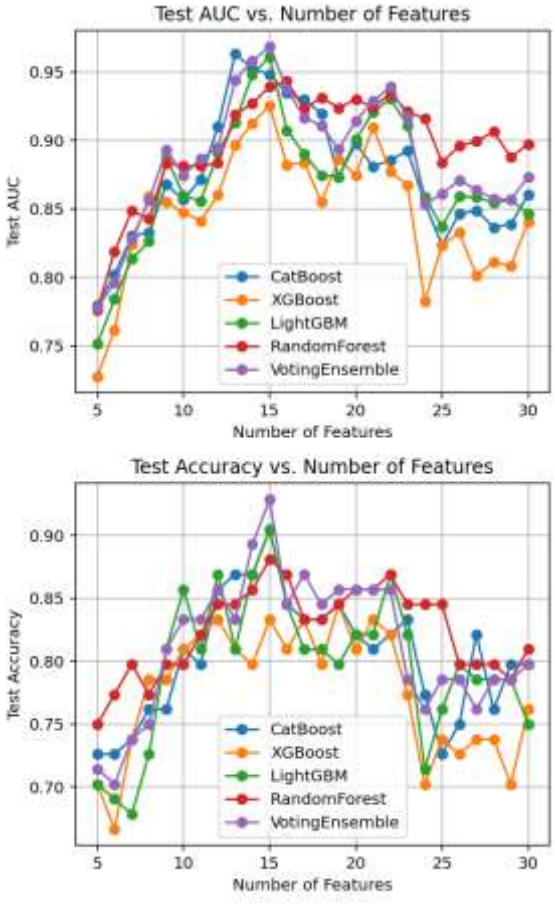

Figure 6. *Accuracy and AUC of each model using different numbers of most important features.*

The models were assessed using accuracy (Acc), AUC, precision, recall, F1 score, and Cohen's kappa, as summarized in Table 3. These metrics provide a comprehensive evaluation of classification performance, discriminative ability, and agreement beyond chance.

Table 3. *Test performance metrics (%).*

Model	ACC	AUC	Precision	Recall	F1 Score	Kappa
CatBoost	90.48	94.82	86.79	97.87	92.00	80.34
XGBoost	83.33	92.52	83.67	87.23	85.42	65.99
LightGBM	90.48	96.09	88.24	95.74	91.84	80.45
RF	88.10	93.90	83.64	97.87	90.20	75.28
VE	**92.86**	**96.84**	**90.20**	**97.87**	**93.88**	**85.34**

The Voting Ensemble (VE) model achieved the highest performance across most metrics, with an accuracy of 92.86%, an AUC of 96.84%, a precision of 90.20%, an F1 Score of 93.88%, and a Kappa of 85.34%. This suggests that combining the strengths of individual models (CatBoost, XGBoost, LightGBM, and RF) through ensemble voting enhances overall predictive performance, particularly in terms of accuracy and robustness (as indicated by the high Kappa score). The VE model also matched the highest recall (97.87%), shared with CatBoost and RF, indicating excellent sensitivity to positive class identification.

LightGBM and CatBoost both exhibited strong performance, each with an accuracy of 90.48%. LightGBM slightly outperformed CatBoost in AUC (96.09% vs. 94.82%) and precision (88.24% vs. 86.79%), while CatBoost achieved a marginally higher recall (97.87% vs. 95.74%). These results highlight the competitive nature of gradient boosting models in handling complex datasets, with LightGBM excelling in distinguishing between classes (higher AUC) and CatBoost maintaining a balance across metrics.

Random Forest (RF) showed robust performance with an accuracy of 88.10% and a high recall of 97.87%, matching CatBoost and VE. However, its precision (83.64%) was the lowest among the models, suggesting a higher rate of false positives. This trade-off indicates RF's strength in capturing true positives but at the cost of reduced specificity compared to other models.

XGBoost recorded the lowest performance across all metrics, with an accuracy of 83.33%, AUC of 92.52%, and Kappa of 65.99%. While still competitive, its lower scores suggest it may be less suited to this specific dataset compared to the other models, potentially due to overfitting or sensitivity to hyperparameter settings.

Additional visualizations provided further insights into the models' performance across different thresholds and error types:

The superior performance of the Voting Ensemble (VE) model suggests that combining predictions from multiple models effectively leverages their individual strengths, leading to improved

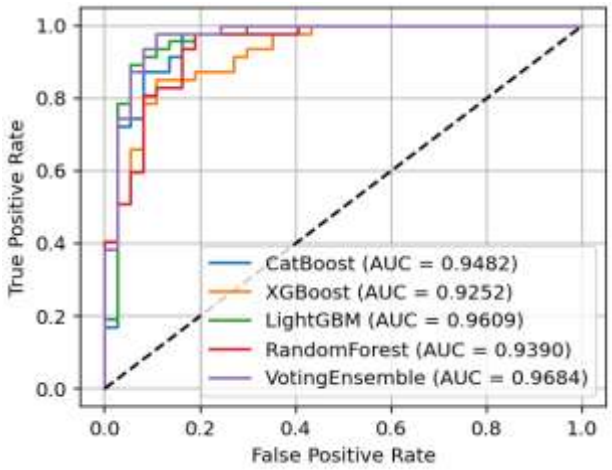

Figure 7. *ROC Curve comparison of the VE model with others models*

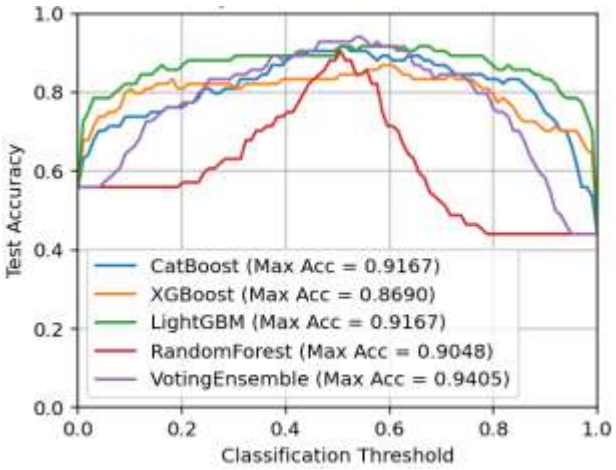

Figure 8. *Accuracy comparison of the VE model with others models*

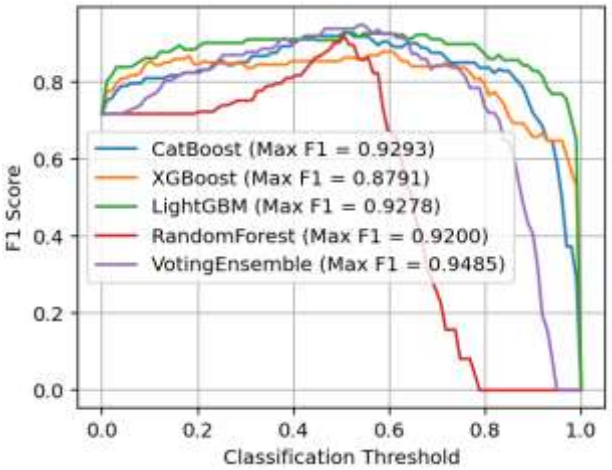

Figure 9. *F1 Score comparison of the VE model with others models*

generalization and robustness. The high Kappa score (85.34%) further confirms VE's reliability in handling class imbalances, as it accounts for agreement beyond chance.

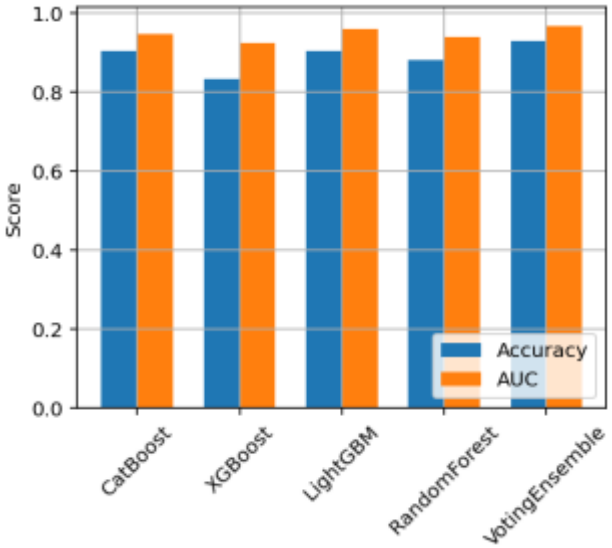

Figure 10. *Accuracy and AUC comparison.*

The AUC scores across all models were consistently high (>92.52%), indicating good discriminative ability between classes. However, VE's slight edge in AUC (96.84%) reinforces its overall superiority. The variation in Kappa scores suggests differences in how well each model handles class imbalance, with VE and LightGBM being the most robust.

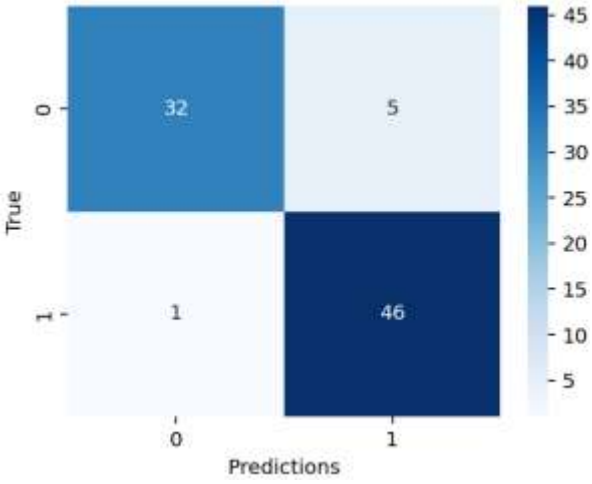

Figure 11. *Confusion matrix of the proposed model using 15 most important radiomics features*

The confusion matrix for VE at the fixed threshold (likely 0.5) showed 48 true positives (TP), 46 true negatives (TN), 3 false positives (FP), and 3 false negatives (FN), yielding an accuracy of 92.86%, precision of 90.20%, recall of 97.87%, and F1 score of 93.88%. These values align with the table, except for Accuracy, which is reported as 92.86% in the table, likely reflecting the maximum accuracy achievable at an optimal threshold. The reported sample size in the matrix (N=84) indicates a potential inconsistency with important features count equal 15, suggesting either a typographical

error or the utilization of a more extensive dataset for this particular analysis.

In summary, the voting ensemble model outperformed individual models, leveraging their collective strengths to achieve superior accuracy, precision, and robustness. LightGBM and CatBoost also demonstrated strong capabilities, making them viable alternatives depending on the specific requirements of the task. Further analysis could explore feature importance, model interpretability, and the impact of hyperparameter tuning to optimize performance further.

5. Conclusions

The study highlights the efficacy of a machine learning approach in predicting MGMT methylation status in glioblastoma (GBM) patients using radiomics features derived from multi-sequence MRI scans. The proposed model's robust performance, with an accuracy of 92.84% and an AUC of 96.84%, underscores its high predictive reliability, making it a promising tool for non-invasive biomarker assessment. The incorporation of important features through multi-modal data analysis significantly enhances the model's effectiveness, offering a valuable alternative to traditional methods. These results emphasize the potential of machine learning to advance precision medicine in GBM, facilitating personalized and informed treatment strategies. Moving forward, validating the model with larger, more diverse datasets and integrating it into clinical workflows will be crucial to maximize therapeutic outcomes for patients with this aggressive brain tumor.

Author Statements:

- **Ethical approval:** The conducted research is not related to either human or animal use.
- **Conflict of interest:** The authors declare that they have no known competing financial interests or personal relationships that could have appeared to influence the work reported in this paper
- **Acknowledgement:** The authors declare that they have nobody or no-company to acknowledge.
- **Author contributions:** The authors declare that they have equal right on this paper.
- **Funding information:** The authors declare that there is no funding to be acknowledged.
- **Data availability statement:** The data that support the findings of this study are available on request from the corresponding author. The data are not publicly available due to privacy or ethical restrictions.

References

[1] Louis, D. N., Perry, A., Wesseling, P., Brat, D. J., Cree, I. A., Figarella-Branger, D., Hawkins, C., Ng, H. K., Pfister, S. M., Reifenberger, G., Soffietti, R., von Deimling, A., & Ellison, D. W. (2021). The 2021 WHO classification of tumors of the central nervous system: A summary. Neuro-Oncology, 23(8), 1231–1251. https://doi.org/10.1093/neuonc/noab106

[2] Hegi, M. E., Diserens, A.-C., Gorlia, T., Hamou, M.-F., de Tribolet, N., Weller, M., Kros, J. M., Hainfellner, J. A., Mason, W., Mariani, L., Bromberg, J. E. C., Hau, P., Mirimanoff, R. O., Cairncross, J. G., Janzer, R. C., & Stupp, R. (2005). MGMT gene silencing and benefit from temozolomide in glioblastoma. New England Journal of Medicine, 352(10), 997–1003. https://doi.org/10.1056/NEJMoa043331

[3] Stupp, R., Mason, W. P., van den Bent, M. J., Weller, M., Fisher, B., Taphoorn, M. J. B., Belanger, K., Brandes, A. A., Marosi, C., Bogdahn, U., Curschmann, J., Janzer, R. C., Ludwin, S. K., Gorlia, T., Allgeier, A., Lacombe, D., Cairncross, J. G., Eisenhauer, E., & Mirimanoff, R. O. (2005). Radiotherapy plus concomitant and adjuvant temozolomide for glioblastoma. New England Journal of Medicine, 352(10), 987–996. https://doi.org/10.1056/NEJMoa043330

[4] Kickingereder, P., Burth, S., Wick, A., Götz, M., Eidel, O., Schlemmer, H.-P., Maier-Hein, K. H., Wick, W., Bendszus, M., Radbruch, A., & Bonekamp, D. (2016). Radiomic profiling of glioblastoma: Identifying an imaging predictor of patient survival with improved performance over established clinical and radiologic risk models. Radiology, 280(3), 880–889. https://doi.org/10.1148/radiol.2016160845

[5] Baid, U., Ghodasara, S., Mohan, S., Bilello, M., Calabrese, E., Colak, E., Farahani, K., Kalpathy-Cramer, J., Kitamura, F. C., Pati, S., Prevedello, L. M., Rudie, J. D., Sako, C., Shinohara, R. T., Wiestler, B., Flanders, A. E., Menze, B., & Bakas, S. (2021). The RSNA-ASNR-MICCAI BraTS 2021 benchmark on brain tumor segmentation and radiogenomic classification. arXiv. https://doi.org/10.48550/arXiv.2107.02314

[6] Sasaki, T., Kinoshita, M., Fujita, Y., Fukai, J., Hayashi, S., Uematsu, Y., Okita, Y., Nonaka, M., Tsuyuguchi, N., Moriuchi, S., Ueda, T., Ozaki, Y., Nakajima, Y., Fujinaka, T., Yoshimine, T., & Kishima, H. (2019). Radiomics and MGMT promoter methylation for prognostication of newly diagnosed glioblastoma. Scientific Reports, 9(1), Article 14435. https://doi.org/10.1038/s41598-019-50849-y

[7] Hajianfar, G., Shiri, I., Maleki, H., Oveisi, M., & Zaidi, H. (2023). Noninvasive O6-methylguanine-DNA methyltransferase status prediction in glioblastoma multiforme cancer using magnetic resonance imaging radiomics features. Journal of

Neuroimaging, 33(1), 104–113. https://doi.org/10.1111/jon.13054

[8] Qian, J., Herman, M. G., Brinkmann, D. H., Laack, N. N., Kemp, B. J., Hunt, C. H., Lowe, V., & Pafundi, D. H. (2020). Prediction of MGMT status for glioblastoma patients using radiomics feature extraction from 18F-DOPA-PET imaging. International Journal of Radiation Oncology, Biology, Physics, 108(5), 1339–1346. https://doi.org/10.1016/j.ijrobp.2020.02.012

[9] Tasci, E., Zhuge, Y., Zhang, L., Ning, H., Cheng, J. Y., Miller, R. W., Camphausen, K., & Krauze, A. V. (2025). Radiomics and AI-based prediction of MGMT methylation status in glioblastoma using multiparametric MRI: A hybrid feature weighting approach. Diagnostics, 15(10), Article 1292. https://doi.org/10.3390/diagnostics15101292

[10] Crisi, G., & Filice, S. (2022). Predicting MGMT promoter methylation of glioblastoma from dynamic susceptibility contrast perfusion: A radiomic approach. Journal of Neuroimaging, 32(3), 448–457. https://doi.org/10.1111/jon.12962

[11] Korfiatis, P., Kline, T. L., Coufalova, L., Lachance, D. H., Parney, I. F., Carter, R. E., Buckner, J. C., Kaufmann, T. J., & Erickson, B. J. (2016). MRI texture features as biomarkers to predict MGMT methylation status in glioblastomas. Medical Physics, 43(6), 2835–2844. https://doi.org/10.1118/1.4948668

[12] Han, Y., Wang, S., Li, J., Zhang, Z., Yang, S., Liu, Y., Zhang, S., Xia, S., Shi, Z., Yan, L. F., & Wang, W. (2018). Non-invasive genotype prediction of chromosome 1p/19q co-deletion by development and validation of an MRI-based radiomics signature in lower-grade gliomas. Neuro-Oncology, 20(6), 808–816. https://doi.org/10.1093/neuonc/nox207

[13] Karabacak, M., Jagtiani, P., Carrasquilla, A., Germano, I. M., & Margetis, K. (2023). Prognosis individualized: Survival predictions for WHO grade II and III gliomas with a machine learning-based web application. npj Digital Medicine, 6(1), Article 200. https://doi.org/10.1038/s41746-023-00948-y

[14] Do, D. T., Yang, R. J., Le, N. Q. K., & Wu, Y. (2022). Improving MGMT methylation status prediction of glioblastoma through optimizing radiomics features using genetic algorithm-based machine learning approach. European Radiology, 32(7), 4560–4570. https://doi.org/10.1007/s00330-021-08503-8

[15] Yu, X., Zhou, J., Wu, Y., Bai, Y., Meng, N., Wu, Q., Jin, S., Liu, H., Li, P., & Wang, M. (2024). Assessment of MGMT promoter methylation status in glioblastoma using deep learning features from multi-sequence MRI of intratumoral and peritumoral regions. Cancer Imaging, 24(1), Article 104. https://doi.org/10.1186/s40644-024-00817-1

[16] Jiang, C., Kong, Z., Liu, S., Feng, S., Zhang, Y., Zhu, R., Chen, W., Wang, Y., Lyu, Y., You, H., Zhao, D., Wang, R., Wang, Y., Ma, W., & Feng, F. (2019). Fusion radiomics features from conventional MRI predict MGMT promoter methylation status in lower grade gliomas. European Journal of Radiology, 121, Article 108714. https://doi.org/10.1016/j.ejrad.2019.108714